Chapter 1

Higgs Production Through b Quark Fusion

In the MSSM, the neutral Higgs bosons are dominantly produced from bottom quark fusion. The Higgs coupling to the fermion depends on m_f/v term, where m_f is the mass of the fermion and v is the vacuum expectation value. Since $m_b \approx 4.7\ GeV$, this Yukawa coupling is weak, which leads to a very small cross section for associated production of Higgs bosons. With the introduction of more than one Higgs doublet in the MSSM, this Yukawa coupling can be enhanced by a factor of $1/cos\beta$, and therefore the cross section associated with bottom quarks can be enhanced by choosing a higher value of $tan\ \beta$. Therefore, for $tan\,\beta > 7$, bottom quark fusion is the dominant process to produce neutral Higgs bosons in the MSSM. In the literature, a number of studies have been carried out about the Higgs production from b quarks. Reference [1] presents a NLO calculation for the total cross section of Higgs pair production via bottom quark fusion ($b\bar{b} \to hh$) at LHC in the SM. A study of supersymmetric QCD corrections for the Higgs pair production via bottom quark has been presented in [2]. References [3] [4] [5] are a few more studies done on heavy quark fusion and references [6], [7] discuss the Higgs boson production in association with single bottom quark. In this study, we focused on the production of neutral Higgs bosons with a bottom quark pair(b and $\bar{b}$) followed by Higgs decay into a pair of bottom quarks. We also consider the Higgs decay channel of $b\bar{b}\tau^+\tau^-$ with τ decay into leptons, jets and some missing energy. These processes are especially interesting because they consist of diagrams with trilinear Higgs coupling which leads to measuring it in the future runs at LHC. Production cross sections of neutral Higgs bosons in MSSM will be mainly discussed in this chapter and numerical results will be presented for MSSM.

1.1 Leading order cross section for $b\bar{b} \to \phi^0\phi^0 + X$ in MSSM

Fig. 1.1 shows the tree level Feynman diagrams which contributes for $b\bar{b} \to \phi^0\phi^0$ in MSSM.

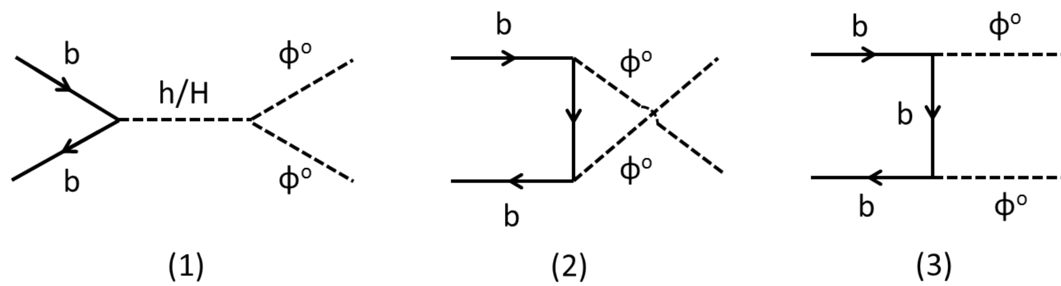

Figure 1.1: The lowest order Feynman diagrams for the production of Higgs boson pair in MSSM from b quark fusion, $\phi^0 = h^0, H^0, A^0$.

For the given Feynman diagrams in the Fig. 1.1, with the initial and final momenta set to be, $b(p_1)\bar{b}(p_2) \to \phi^0(p_3)\phi^0(p_4)$, and $p_1 + p_2 = p_3 + p_4$, the cross section can be simply written as,

$$\sigma_{LO} = \int dx_1 dx_2 [b(x_1)\bar{b}(x_2) + \bar{b}(x_1)b(x_2)] \times \widehat{\sigma}_{LO}(b\bar{b} \to \phi^0\phi^0) \qquad (1.1)$$

where $b(x)$ and $\bar{b}(x)$ are the LO parton distribution functions for the bottom quarks and $\widehat{\sigma}_{LO}$ is the parton level cross section for $(b\bar{b} \to \phi^0\phi^0)$. The Parton level differential cross section over the two body phase space can be written as,

$$\frac{d\sigma}{d\Omega} = \left(\frac{\hbar c}{8\pi}\right)^2 \frac{S\,|M|^2}{(E_1+E_2)^2}\frac{|p_f|}{|p_i|} \tag{1.2}$$

Here, $|p_f|$ is the magnitude of either outgoing momentum and $|p_i|$ is the magnitude of either incoming momentum. S is a product of statistical factors. M is the average amplitude for the process and ,

$$|M|^2 = \left(\frac{1}{3}\,\frac{1}{3})\right)\left(\frac{1}{2}\,\frac{1}{2})\right)\sum_{spin,\,color}|M_0|^2$$

The amplitude for each diagram can be written in the following form.

$$M_s^0 = \left(\frac{ig_{hbb}g_{h\phi\phi}}{s-{M_h}^2+iM_h\Gamma_h} + \frac{ig_{Hbb}g_{H\phi\phi}}{s-{M_H}^2+iM_H\Gamma_H}\right)\left(\overline{v}(p_2)P_L u(p_1) + \overline{v}(p_2)P_R u(p_1)\right)\delta_{\alpha\beta}$$

$$M_t^0 = \frac{g^2_{\phi bb}}{t}\left(\overline{v}(p_2)\not{p_3}P_L u(p_1) + \overline{v}(p_2)\not{p_3}P_R u(p_1)\right)\delta_{\alpha\beta}$$

$$M_u^0 = -\frac{g^2_{\phi bb}}{u}\left(\overline{v}(p_2)\not{p_3}P_L u(p_1) + \overline{v}(p_2)\not{p_3}P_R u(p_1)\right)\delta_{\alpha\beta}$$

where α, β are color indices for initial b and $\overline{b}$, $P_{R,L} = (1 \pm \gamma_5)/2$ and s, t, u are Mandelstam variables defined as

$$s = (p_1 + p_2)^2$$

$$t = (p_1 - p_3)^2$$

$$u = (p_2 - p_3)^2$$

The $g_{\phi bb}$ denotes the Yukawa couplings and $g_{h\phi\phi}$ and $g_{H\phi\phi}$ are trilinear Higgs couplings given in Appendices A and B. Γ_h is the decay width of the Higgs boson. The total amplitude was calculated by squaring the corresponding spin and color averaged matrix elements including interference terms.

1.2 Calculation Tools

The cross section is calculated using the NWA for $pp \to \phi^0\phi^0 \to b\bar{b}b\bar{b} + X$ via $b\bar{b} \to \phi^0\phi^0$ where, $\phi^0 = h^0, A^0, H^0$ for MSSM. Transition amplitudes were calculated both analytically and by using MadGraph for comparison purposes. The masses of the quarks for coupling terms were chosen to be the NLO running masses which are calculated at the pole masses of $m_t = 173.1$ GeV and $m_b = 4.7$ GeV. The renormalization scale is set to be $\mu_R = m_\phi/2$ for the calculation of strong coupling and running masses. Finally we simulate the pp collisions by applying the parton distribution functions of MSTW2008 with the factorization scale $\mu_F = m_\phi/2$. The light Higgs and Heavy Higgs masses and mixing angles were calculated using FeynHiggs for different SUSY parameters as discussed in Chapter 2. All other masses, couplings, cuts and other constants were calculated the same way as discussed in Chapter 2 for the gluon fusion processes.

1.3 Numerical Results

1.3.1 Standard Model

In the SM, bottom quark fusion can produce Higgs pairs at a small rate compared to gluon fusion. However, here we evaluate the leading order cross section for the production of Standard Model Higgs pair as an initiation for the extended models. Leading order cross sections evaluated for Higgs pair production from $b\bar{b}$ in the SM are given in Table 1.1. The cross section for the complete processes after the decay of the Higgs is also included in this table. The cuts explained in the gluon fusion were used here for the final state particles.

	$M_h = 123$ GeV	$M_h = 126$ GeV	$M_h = 129$ GeV
$\sigma(b\bar{b} \to hh)$	8.96×10^{-2}	8.55×10^{-2}	8.16×10^{-2}
$\sigma(b\bar{b} \to hh \to b\bar{b}b\bar{b} + X)$	3.70×10^{-2}	3.06×10^{-2}	2.47×10^{-2}

Table 1.1: Leading order cross section in fb for Standard Model Higgs pair production via b quark fusion. Cross sections for the complete processes after Higgs decay are also given.

1.3.2 Higgs pair production from b quark fusion in MSSM

Higgs pair production via bottom quark fusion in the MSSM is more interesting due to enhanced Yukawa couplings in two Higgs doublet Models. These enhanced Higgs pair production rates are significant in exploring trilinear Higgs coupling at the LHC. Hence the calculation of production cross sections through b quark at LHC is motivated by MSSM. The cross sections for $pp \rightarrow \phi^0\phi^0 \rightarrow b\bar{b}b\bar{b} + X$ and $pp \rightarrow \phi^0\phi^0 \rightarrow b\bar{b}\tau^+\tau^- \rightarrow b\bar{b}l_\tau j_\tau + X$ were evaluated at $\sqrt{s} = 14$ TeV for $\phi^0 = A^0, h^0, H^0$, the three neutral Higgs bosons in MSSM. Fig. 1.2 shows the production cross sections of the pseudo scalar as a function of free parameter M_A for two $tan\ \beta$ values. Production cross sections in the MSSM via $b\bar{b}$ are higher compared to the cross sections in the SM Higgs production with the introduction of $tan\ \beta$. The values increase significantly with the increasing value of $tan\ \beta$.

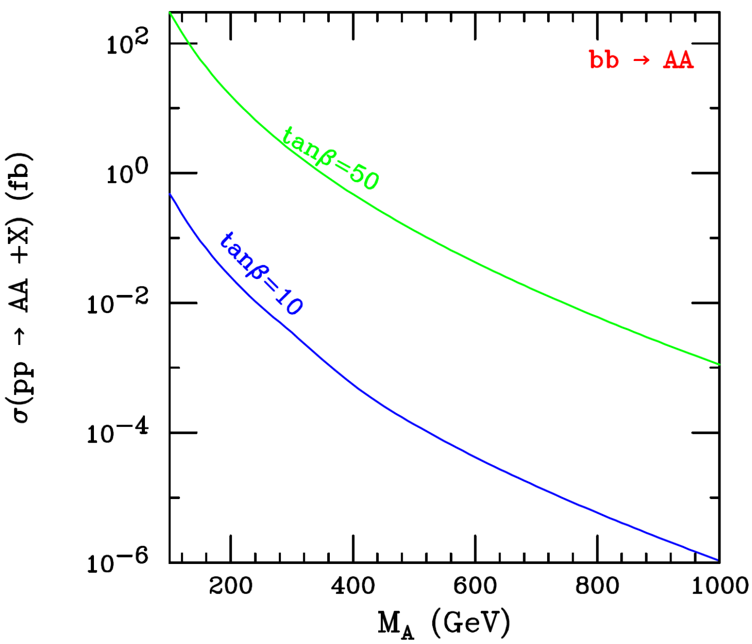

Figure 1.2: Leading order cross sections for the pair production of pseudo scalars from bottom quark fusion versus mass M_A(solid line). Green represents $tan\ \beta = 50$ and blue represents $tan\ \beta = 10$.

Pseudoscalars produced from $b\bar{b}$ collisions that decay into $b\bar{b}$ was considered and

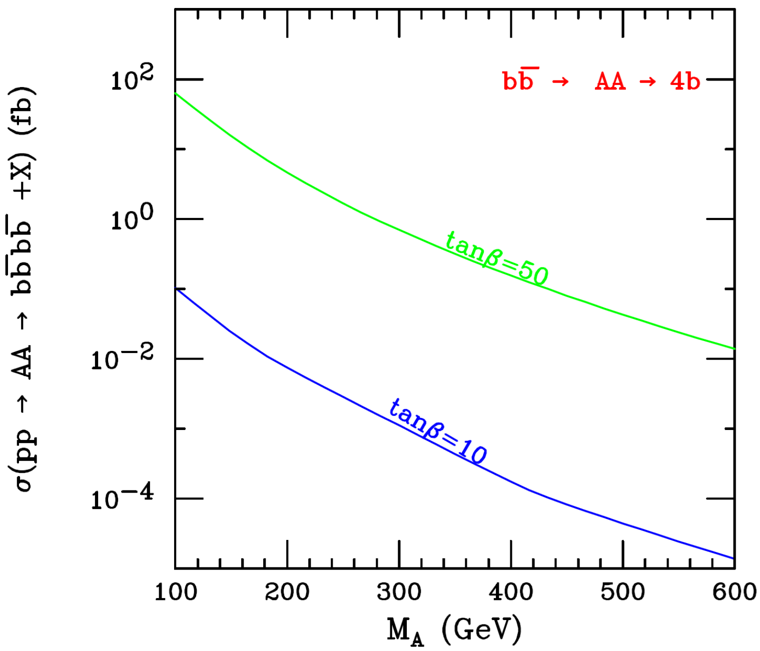

Figure 1.3: LO cross sections evaluated for $b\bar{b}b\bar{b}$ final state via pseudo scalars from b quark fusion(solid line). Green represents $tan\ \beta = 50$ and blue represents $tan\ \beta = 10$.

$\sigma(pp \to A^0A^0 \to b\bar{b}b\bar{b} + X)$ vs mass for the pseudo scalar was plotted in Fig. 1.3. The cross sections from $b\bar{b}$ are very close to the cross sections evaluated from gluon fusion even with smaller PDFs for b quark compared to gluon PDFs. Fig. 1.4 presents the leading order cross sections for the $b\bar{b}lj_\tau$ final state via pseudoscalars produced from b quark fusion. Cross sections are smaller compared to 4b final state though the significance of background vs signal will be better due to a cleaner background in this case.

As discussed in Chapter 2, since the MSSM light Higgs should have a mass close to the SM Higgs, setting $tan\beta$ to very high values is not meaningful in this case. Cross

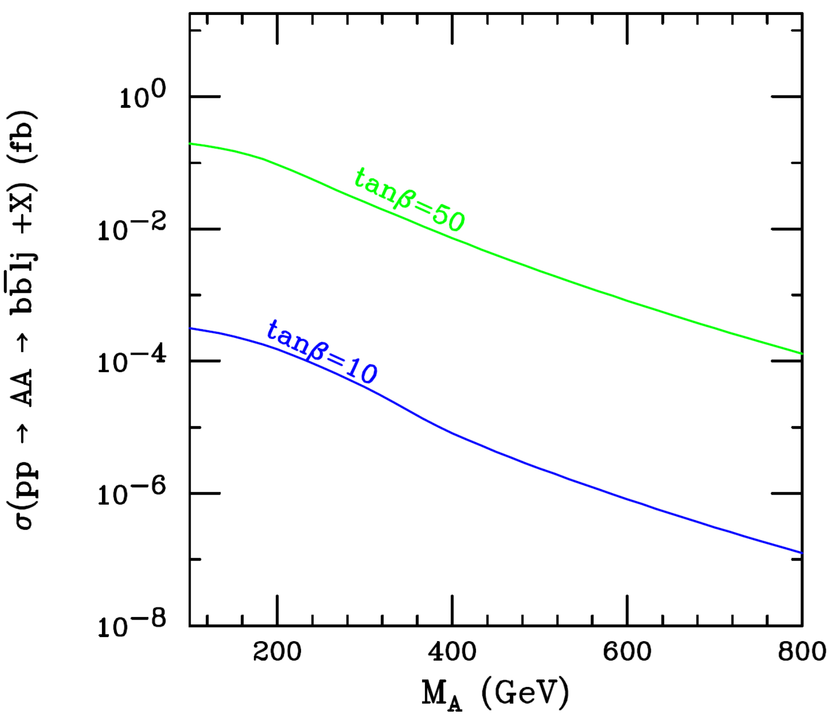

Figure 1.4: Leading order cross section for the production of the pseudoscalar(A^0) followed by $A^0A^0 \to b\bar{b}\tau^+\tau^- \to b\bar{b}lj_\tau + \not{E_T}$.

sections were evaluated for $tan\beta = 5$ and $tan\beta = 10$ for the light Higgs production via $b\bar{b}$ fusion with the Higgs decaying into $b\bar{b}$. Leading order cross sections for production of light Higgs bosons were evaluated for $4b$ and $bb\tau\tau$ channels. The results are presented in the figures 1.5 and 1.6 respectively.

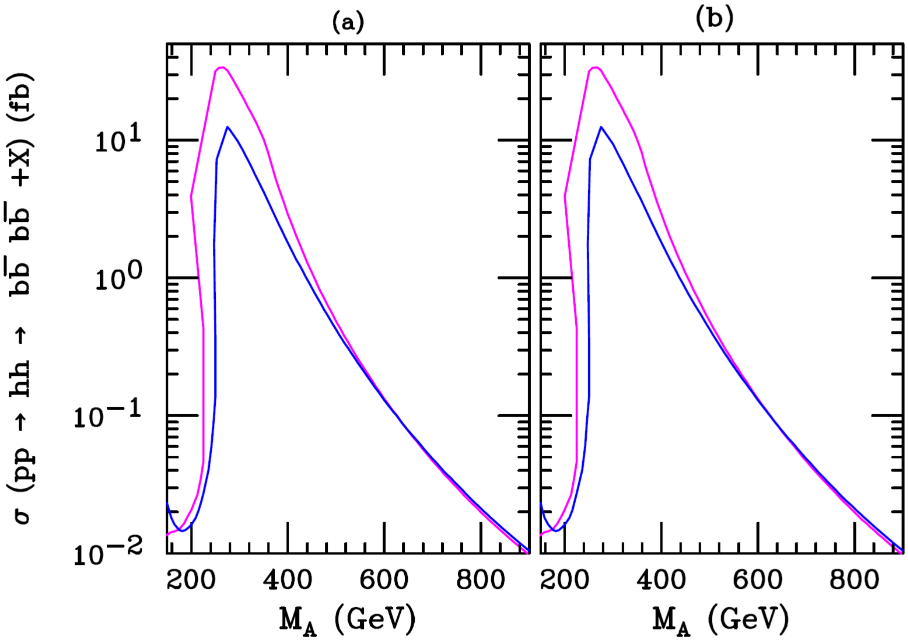

Figure 1.5: LO cross sections for $pp \to \phi\phi \to b\bar{b}b\bar{b} + X$ via b quark fusion. ϕ is the MSSM light Higgs. Magenta represents $tan\ \beta = 5$ and blue represents $tan\ \beta = 10$ b quark fusion. (a) For light Higgs produced with $Msusy = 1000\ GeV$, $X_t = 2000\ GeV$ (b) For light Higgs produced with $Msusy = 2000\ GeV$, $X_t = (\sqrt{6} * MSusy)$.

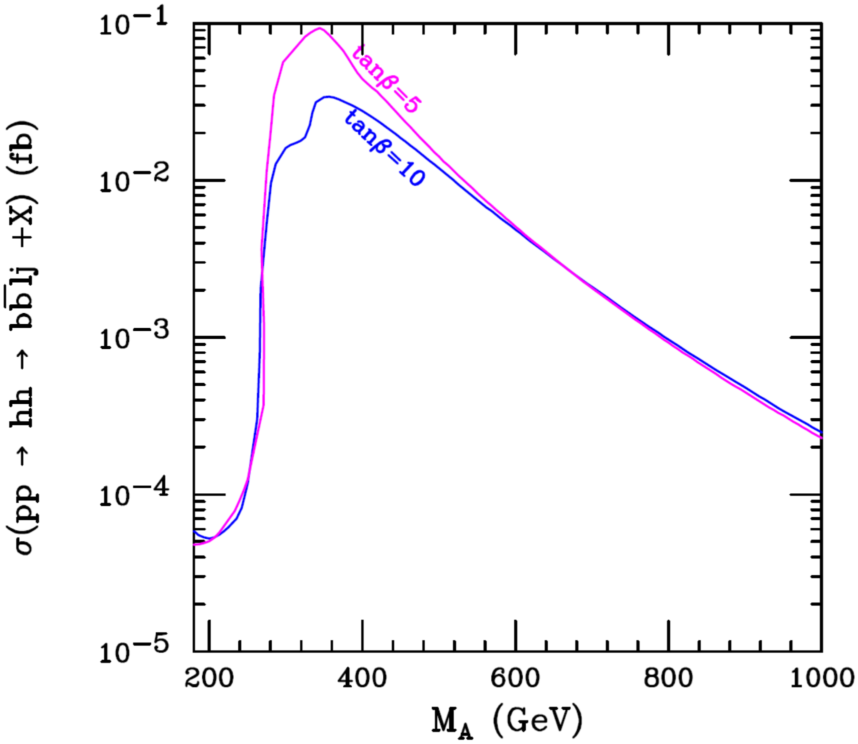

Figure 1.6: LO cross section for the process $pp \to \phi\phi \to b\bar{b}\tau^+\tau^- \to b\bar{b}lj_\tau + \not{E}_T + X$ via $b\bar{b}$ fusion as a function of M_A. MSSM light Higgs masses were evaluated for $Msusy = 2000$ GeV and $X_t = \sqrt{6} \times Msusy$. Magenta represent $tan\ \beta = 5$,blue represent $tan\ \beta = 10$.

References

[1] S. Dawson, C. Kao, Y. Wang, and P. Williams, Physical Review D **75**, (2007).

[2] S. Dawson, C. Kao, and Y. Wang, Physical Review D **77**, (2008).

[3] D. Dicus and S. Willenbrock, Phys. Rev. D **39**, (1989).

[4] D. Dicus, T. Stelzer, Z. Sullivan, and S. Willenbrock, Phys. Rev. D **59**, (1999).

[5] C. Balazs, H. He, and C. P. Yuan, Phys. Rev. D **60**, (1999).

[6] C. Kao, S. Sachithanandam, J. Sayre, and Y. Wang, arXiv:0908.1156[hep-ph] **2**, (2009).

[7] C. Kao, D. A. Dicus, R. Malhotra, and Y. Wang, arXiv:0711.0232[hep-ph] **1**, (2007).